Applied Thermal Engineering 219 (2023) 119446

Contents lists available at ScienceDirect

Applied Thermal Engineering

journal homepage: www.elsevier.com/locate/apthermeng

ELSEVIER

Research Paper

Overshoot temperature control on evaporator wall of loop heat pipe for space vehicle thermal control through bypass line under high thermal load

Cheong Hoon Kwon [a], Eui Guk Jung [b,*]

[a] Division of Energy Engineering, Kangwon National University, Kangwon-do 25913, Republic of Korea
[b] School of Mechanical System Engineering, Kangwon National University, Kangwon-do 25913, Republic of Korea

ARTICLE INFO

Keywords:
Loop heat pipe
Flat evaporator
Overshoot temperature control
Bypass line
Sintered metal wick
Start up

ABSTRACT

This paper presents the experimental results of controlling an evaporator wall temperature overshoot problem under a high thermal load by applying a bypass line to the loop heat pipe (LHP). To solve the overshoot problem during the LHP start-up, any nucleation bubbles generated on the wick surface should be removed from the vapor channel as soon as possible. In special cases, a serious evaporator wall temperature overshoot problem at high thermal loads can cause start-up failure. The LHP must be operated stably within an appropriate temperature range during start-up because any sudden rise in the evaporator wall temperature may cause serious damage to the temperature control target. To control the evaporator wall temperature overshoot of the LHP with a flat evaporator and sintered metal wick, a bypass line was installed between the evaporator and the liquid reservoir. The bypass line was integrated into the LHP using a sintered metal wick and flat evaporator, of dimensions (width and length) 40 × 50 mm. The body of the LHP was made of stainless steel, and distilled water was used as the working fluid. The vapor generated in the evaporator was supplied to the vapor transport tube through inverted axial trapezoidal grooves. The inner diameters of the liquid and vapor transport tubes were 2 mm and 4 mm, respectively, and both tubes were 0.5 m long. The input thermal load ranged up to 270 W for a coolant temperature of 10 °C. The LHP was aligned at a favorite tilt angle of 15°, where an evaporator wall temperature overshoot was observed. The experimental results demonstrated the ability of the bypass line to effectively control the evaporator wall temperature overshoot during start-up under high thermal loads.

1. Introduction

Loop heat pipes (LHPs) are promising two-phase heat transfer devices that use the latent heat of evaporation and condensation of the working fluid and are considered to be competitive solutions for electronic component cooling and spacecraft thermal control applications. Since the LHP was developed by Maidanik in the 1970 s, reliable heat transfer performance has been proven for aerospace and military spacecraft thermal control applications and the application of LHPs has been expanded and extended to terrestrial applications [1]. As terrestrial electronic components have become smaller, thermal energy generation per unit area has increased, with heat pipes or LHPs being recommended as solutions to technical difficulties in thermal control. Moreover, in recent years, fossil fuels in the automobile industry have been rapidly replaced by lithium-ion [2,3] or hydrogen batteries. A heat pipe or LHP has the potential to solve the problem of heat generation in fuel cells. For this reason, studies on the application of heat pipes and LHPs for the thermal control of fuel cells are being actively conducted [4].

Although an LHP is a high-performance heat transfer device, there are some difficulties in its design, fabrication, and operation. First, the driving force of the LHP is governed by the capillary pressure generated in fine capillaries. In a typical LHP operation, under operating conditions where the evaporator is placed above the condenser, sufficient capillary pressure must be supplied to allow the liquid to overcome gravity and return to the evaporator normally. Therefore, a sintering technology capable of precisely controlling the porosity is needed for the production of capillary structures. Second, start-up becomes impossible when the thermal load is lower than the minimum starting thermal load [5]. The capillary structure, the optimal LHP tubing system, and heat leakage protection technology from the vapor removal channel to the compensation chamber are required to further lower the minimum starting thermal load. Third, the evaporator wall temperature overshoot during LHP start-up under high thermal loads remains a problem [6]. In previous studies, efforts were made to address these difficulties. Maidanik [7] proposed including an auxiliary heater to achieve a quasi-stable

* Corresponding author.
E-mail addresses: chkwon2@kangwon.ac.kr (C. Hoon Kwon), egjung@kangwon.ac.kr (E. Guk Jung).

https://doi.org/10.1016/j.applthermaleng.2022.119446
Received 26 December 2021; Received in revised form 15 September 2022; Accepted 3 October 2022
Available online 8 October 2022
1359-4311/

Nomenclature

BOM	bypass operation mode
M	mass of working fluid
NOM	normal operation mode
Q	thermal load (W)
R	thermal resistance (°C/W)
t	time (s)
T	temperature (°C)
V	volume (ml)
α	fill charge ratio (based on the internal volume of the evaporator)
ρ	density (kg/m^3)
φ	tilt angle (degree)
bl	bypass line (or auxiliary loop)
c	condenser
ci	condenser inlet
co	condenser outlet
cool, i	coolant inlet
cool, o	coolant outlet
e	evaporator
ew	evaporator wall (average)
ev	evaporator vapor
eo	evaporator outlet
ei	evaporator inlet
g	groove
in	inlet, input
l	liquid
ll	liquid line
res.	liquid reservoir
r	reservoir
s	steady state
start	start-up
Sys	system
th	thermal
v	vapor
vl	vapor line
w	wall or wick
wick.i	wick inlet

LHP temperature for a given thermal load range using the active temperature control of a compensation chamber. Boo and Jung reduced the minimum start-up thermal load [5], improved the steady-state heat transfer performance [8] and eliminated overshoot on the evaporator wall temperature [9] by installing a bypass line between the evaporator and the liquid reservoir. In their study, the positive and negative effects of the bypass line during LHP start-up and steady-state were demonstrated. Mo *et al.* [10,11] adopted an electro-hydrodynamic technique to shorten the start-up period by inducing additional pressure, and consequently enhanced the thermal performance of the LHP. In their study, the reduction in start-up time improved the heat transfer performance by reducing the LHP evaporator wall temperature during steady-state operation. Liu *et al.* [12] proposed an LHP with vapor-driven jet injection to attenuate the negative effects of heat leakage on compensation and to improve the performance of LHPs, significantly improving the heat transfer performance. A bypass line between the vapor removal groove and liquid reservoir to improve the start-up and steady-state heat transfer performance of the LHP was first proposed by Jung and Boo [5,8,9]. In their study, the results showed that the overshoot problem for the evaporation wall temperature encountered during start-up was completely solved by the application of the bypass line. Thereafter, Liu *et al.* [13] installed a bypass line between the vapor and liquid transfer tubes and experimentally measured the effect of the bypass line on the start-up and steady-state performance of the LHP. Jung and Boo completely solved the overshoot problem on the evaporator wall temperature under a moderate thermal load by applying a bypass line during LHP start-up [9].

The overshoot problem itself is caused by nucleation bubbles that inhibit the convection mechanism, which in turn interfere with heat transfer from the evaporative wall to the working fluid [14,15]. Depending on the operating environment of the LHP, the nucleation bubbles rapidly undergo a phase change and are removed from the evaporator, thereby preventing the overshoot problem [9]. Owing to the overshoot problem, the vapor or liquid in the vapor removal groove may overheat, causing a start-up delay or failure. As the input thermal load increases, the overshoot becomes more severe, making it impossible to increase the input thermal load. Consequently, it may be impossible to ensure thermal stability of the heat source components.

This study was conducted as an extension of previous studies [5,8,9,16], in which a description of the operating principle of the bypass line can be found. The basic concept of the bypass line was derived from a literature review [14,15,17,18]. As discussed in detail in these references, the phase-change interface is located in the contact region of the capillary wick and the vapor removal groove at low thermal loads. However, under high thermal load, the dry zone expands inside the wick structure because the vapor–liquid interface recedes into the capillary structure as shown in Fig. 1(a). In an LHP with a bypass line, the bypassed vapor exerts a push on the liquid in the reservoir toward the wick–wall interface. Owing to the higher temperature and pressure of the bypassed vapor, the phase-change interface moves to the wick–wall interface under the same high thermal load as shown in Fig. 1(b). As a result, the reduced dry zone reduces the thermal resistance and improves the heat transfer performance. Essentially, the bypass line can control the local maximum temperature as well as the local temperature difference on the evaporator wall.

The possibility that the bypass line could function as a safety device to control temperature overshoot during LHP start-up was suggested in this study. That is, if the bypass line is designed to be activated only when the temperature of the outer wall of the evaporator rises abnormally during start-up or in a steady-state condition, the bypass line can function as an emergency safety device. This study differs from previous studies [5,3,9,16] in that the main purpose of this study was to investigate the applicability of the bypass line as an emergency safety device for the LHP.

In a previous study [9], the start-up performance of an LHP was compared in the normal operating mode (NOM)—in which the bypass line was not activated—and the bypass operating mode (BOM)—in which the bypass line was activated under a moderate thermal load of 160 W or less—and the temperature overshoot was completely eliminated by the bypass line. However, as shown in a previous study [8], since the start-up of the LHP was impossible due to extreme temperature overshoot under a high thermal load, the LHP was started by applying the BOM and was converted to the NOM after reaching a steady state, after which the steady-state performance for the two modes was compared. During start-up of the LHP at high thermal loads, the temperature overshoot can become severe because there is insufficient working fluid corresponding to the high heat transfer rate. To solve the start-up problem under a high thermal load—when the wall temperatures exceed a certain level owing to the evaporator wall temperature overshoot after start-up in the NOM—the response of the temperature overshoot on activation of the bypass line needs to be investigated experimentally. The high thermal load in this study was defined as the thermal load in which the maximum wall temperature of the evaporator exceeds 100 °C in the steady state.

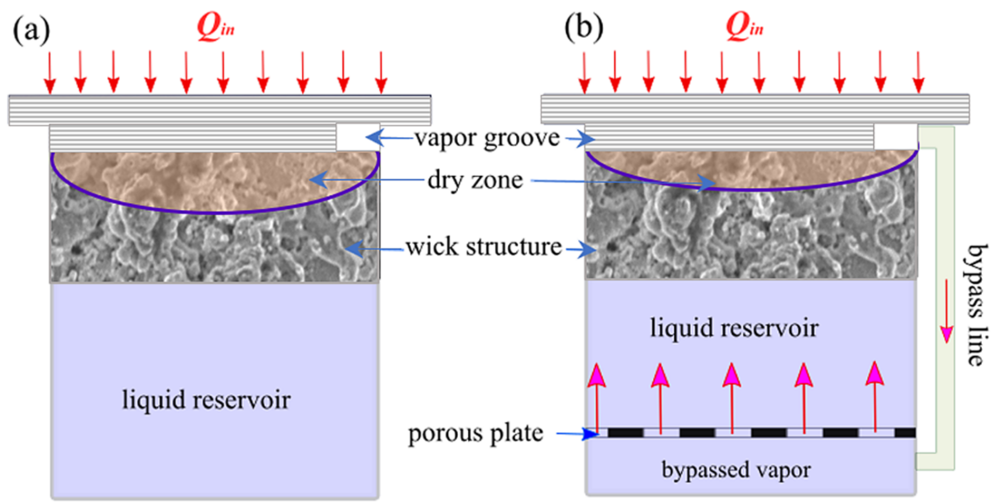

Fig. 1. Schematic of the liquid–vapor interface inside the wick structure under high heat flux: (a) normal operation mode (NOM), and (b) bypass-line operation mode (BOM).

The concept of bypass line in LHP is very attractive because it is a passive method that does not require any additional power consumption or complicated manufacturing process. The effective results of bypass line on start-up and steady-state heat transfer performance of LHP have been provided in previous studies [5,8,9,16]. In particular, detailed experimental results on the thermal performance of LHPs with polypropylene wicks under bypass line operation can be referred to through literature [16]. In their paper, three effective effects of the bypass line on the heat transfer performance of the LHP are experimentally presented, and the useful function of the bypass line on the thermal performance of the LHP is described in detail.

Although several previous studies [5,9,16] have experimentally demonstrated the advantages of bypass lines in LHP start-up, they mainly focused on the start-up transient process, and the test cases were limited to the low thermal load range. Thus far, there has been no experimental investigation on the effect of the bypass line in controlling the local temperature overshoot in the evaporator during the start-up transient period of the LHP under high thermal loads, to obtain a thorough understanding of the related phenomenon. This study aims to perform an in-depth analysis and discuss the usefulness of the bypass line as a passive method for controlling the evaporator temperature overshoot of LHP based on the experimental results under high thermal load. The purpose of this study is to solve the problem of temperature rise by using the bypass line only when there is temporary overheating, such as temperature overshoot during the start-up process of the LHP. The possibility of the LHP functioning as an auxiliary safety device for the bypass line in the start-up or steady-state operation of the LHP system is proposed in this study.

2. Methods: experimental setup and procedure

The LHP experimental system incorporating the bypass line applied in this study is the same as that in the literature [8,9], in which the components and geometric sizes of the LHP are provided in detail. During start-up under a high thermal load, normal operation of the LHP becomes impossible when the evaporator wall temperature overshoot increases rapidly.

In a previous study, start-up in the NOM was performed only for thermal loads where the temperature overshoot was lower than 200 °C, and the effective input thermal load range was found to be less than 160 W. The temperature limit can be arbitrarily defined as appropriate to protect the LHP components, to prevent degradation of the working fluid performance and damage to the heat source components due to overheating. When the input thermal load exceeded 160 W under the NOM, start-up of the LHP could not be successfully executed as the evaporator wall overshoot temperature exceeded 200 °C, the temperature overshoot becoming more severe as the input thermal load increased.

The purpose of this work is to measure whether control is possible by switching to the BOM to reduce the temperature overshoot when the temperature overshoot it exceeds 200 °C after start-up in the NOM under the condition of applying a thermal load of more than 160 W. Consequently, the function of the bypass line as an LHP system safety device was investigated—specifically, temperature control using the bypass line when the temperature temporarily increased abnormally during start-up or steady state operation.

Fig. 2 shows a schematic of the LHP system (including the thermocouple location) used in this experimental work. As shown in Fig. 2, a rectangular flat evaporator and condenser were connected by vapor and liquid transport tubes. Conventional evaporators are commonly manufactured in cylindrical types. However, because the thermal resistance of the flat evaporator is lower than that of the cylindrical evaporator, the flat evaporator shows excellent isothermal performance [25]. A liquid reservoir (often called a compensation chamber) was integrated with a rectangular plane evaporator and a capillary wick structure sintered with metal powder. The flat evaporator had dimensions (height, width, and length) of 30, 40, and 50 mm, respectively.

The operation of the LHP is based on the capillary force produced in the fine pore of the wick structure. Although the wick structure is mostly composed of nickel or titanium, the heat transfer performance of an LHP using a sintered metal made of an alternative material such as stainless steel has been actively studied [25–28]. Stainless steel powder has the disadvantage of being manufactured in a relatively high-temperature environment compared to nickel or titanium; however, it has the advantage of being inexpensive. Previous studies [26–29] have investigated stainless-steel as an economical alternative to nickel or titanium for use with sintering technology. The capillary wick structure applied to the LHP in this study was sintered with 316L stainless steel powder having a porosity of 49.4 %. The wick structure had a pore size of 2.3 μm and a thickness of 6 mm. Fig. 3 depicts the scanning electron microscopy (SEM) images of the wick. In the operation of the LHP, the design of the wick structure plays a key role in obtaining its stable operation and excellent heat transfer performance. However, the purpose of this study was to experimentally investigate the function of the bypass line as a way to eliminate or alleviate the overshoot for the evaporation wall temperature, which inherently occurs in the operation of LHP. In particular, the main purpose was to propose a new possibility of controlling temperature overshoot through the intermittent opening of the

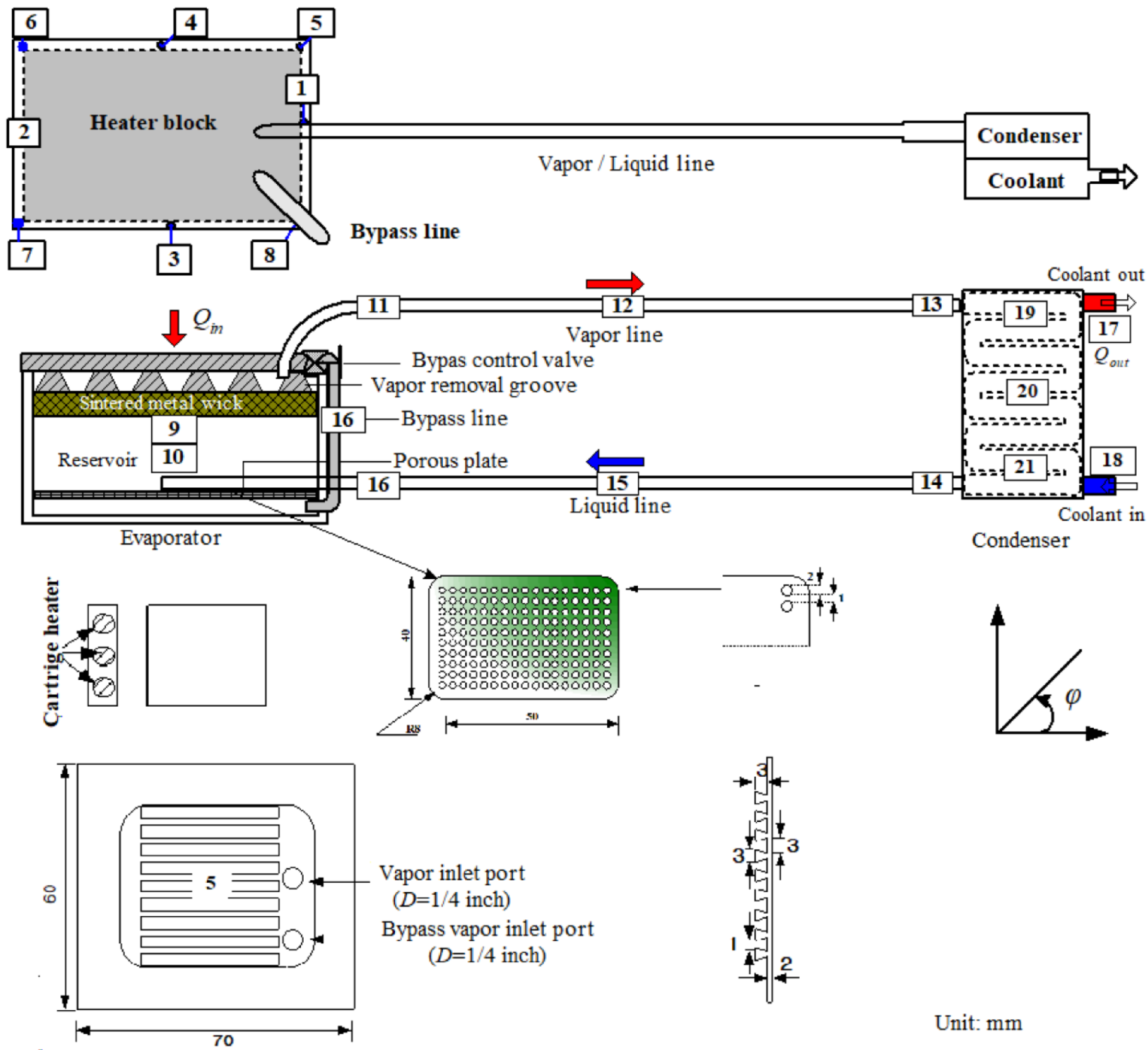

Thermocouple locations: 1–8: evaporator wall (T_w), 9: wick inlet ($T_{wick.i}$), 10: liquid reservoir (T_R), 11: evaporator outlet (T_{evo}), 12: vapor line (T_{vl}), 13: condenser inlet (T_{ci}), 14: condenser outlet (T_{co}), 15: liquid line (T_{ll}), 16: evaporator inlet (T_{ei}), 17: coolant inlet ($T_{cool.\,i}$), 18: coolant outlet ($T_{cool.o}$), 19–21: condenser wall (T_{cw}), 22: bypass line tube (T_{bl})

Fig. 2. Schematic of the LHP fabricated in this study and location of thermocouples [16].

bypass valve. Therefore, topics related to sintered metal fabrication technology are beyond the scope of this study.

Fig. 4 presents the porosity, permeability, and pore size of the capillary wick used in this study with respect to pressure. The sintering temperature is 700 °C. As shown in Fig. 5, when the sintering pressure increases, the permeability, porosity, and pore size decrease simultaneously. In general, the smaller the pore size, the greater the capillary force that can be obtained; however, there are disadvantages in that the porosity and permeability are reduced. Therefore, the wick used in this study was manufactured based on a pressure of 50 MPa. Based on this pressure, the porosity, permeability, and pore size of the wick structure were measured to be 49.4 %, 2.5 milidarcy, and 2.3 μm, respectively.

The effective heating area of the evaporator was 35 × 35 mm, and a heater block comprising three cartridge-type heaters was used as the heat source. The vapor passages inside the evaporator were grooved into nine trapezoidal shapes. Fig. 5 shows a photo of the LHP assembly of this experiment with a flat evaporator attached to a bypass line. The bypass line connected the liquid reservoir and the vapor removal channel outlet of the evaporator, having the same diameter as the vapor transfer tube. In particular, to facilitate the disassembly and installation of the bypass line, a part of the bypass line was applied with a copper tube. A metering valve was installed at the center of the bypass line to control the flow rate of the bypassed vapor. A porous plate was installed to evenly distribute the bypassed vapor inside the liquid reservoir and to minimize the disturbance of the working fluid in the evaporator.

As shown in Fig. 2, a porous plate was installed 7 mm above the base of the liquid reservoir. A large number of small circular holes of diameter 1 mm were machined into the porous plate, the surface opening ratio being 35 % of the total plate area. The bypassed vapor (usually in a superheated state), passes through a small hole in the perforated plate, and is mixed with the supercooled liquid inside the liquid reservoir and condensed. As shown in Figs. 1 and 2, during this process, the relatively high pressure bypassed vapor pushes the liquid inside the liquid reservoir toward the capillary structure. Consequently, the bypassed vapor improves the liquid saturation inside the wick structure near the heating wall of the evaporator, protecting the wick structure from dryness [8].

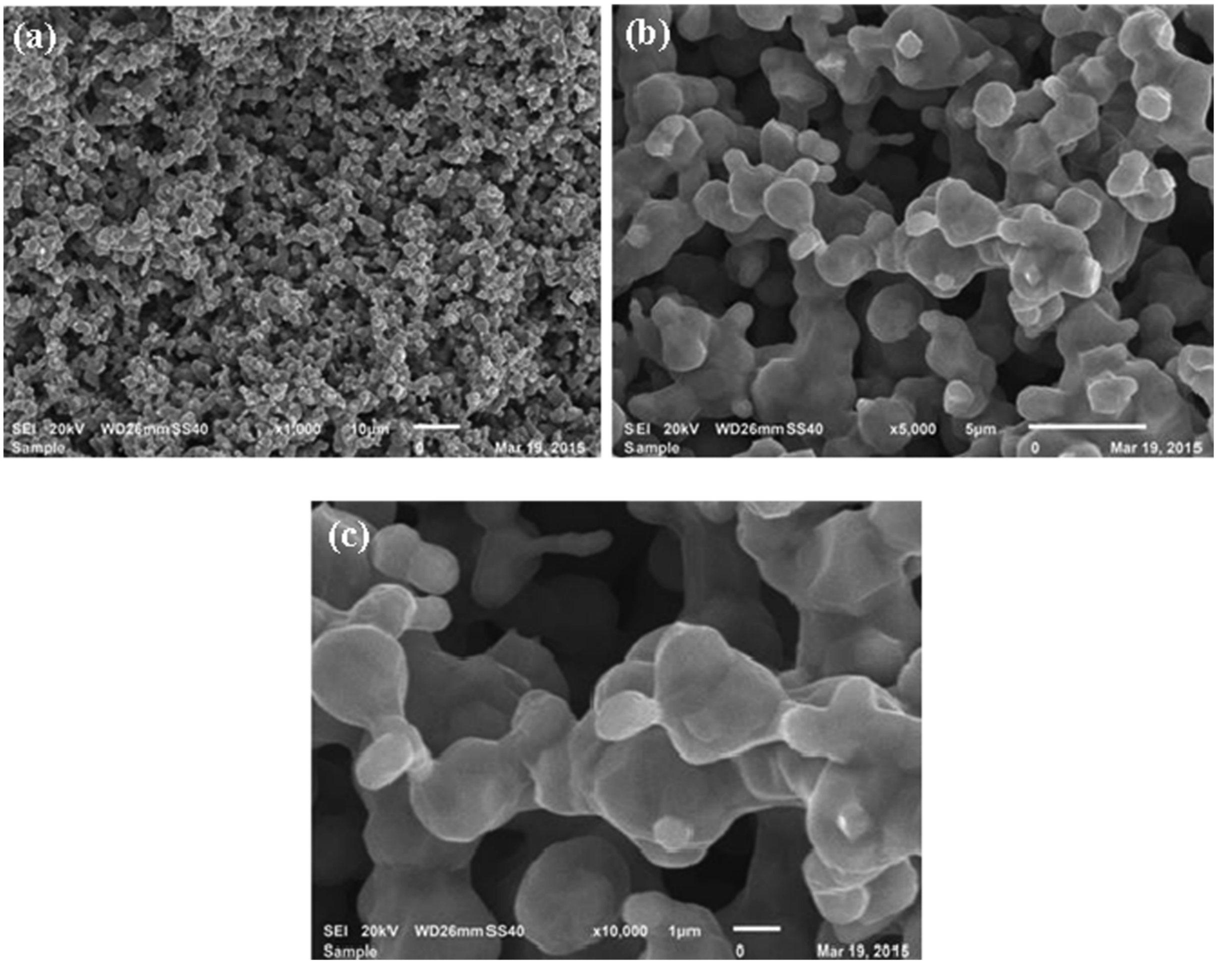

Fig. 3. SEM images of the stainless steel sintered porous wick structure having a pore size of 2.3 μm, with normal magnifications of (a) 1000 times, (b) 5000 times, and (c) 10,000 times.

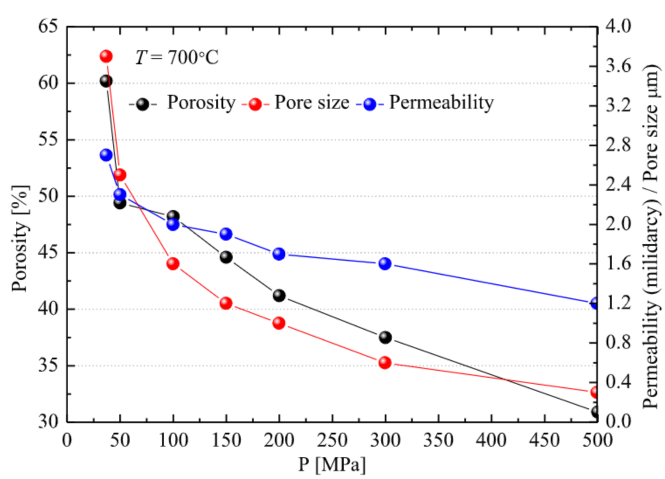

Fig. 4. Variation of porosity, pore size and permeability of the sintered metal wick according to pressure change.

The planar dimension of the condensing section with 10 serpentine channels for the cooling source circulation was 4 × 5 mm. The inner diameters of the liquid and vapor transport tubes were 2 and 4 mm, respectively, their lengths being equal to 500 mm.

Distilled water was selected as the working fluid, and the fill charge ratio of it (α = 47.8 %) was determined using Eq. (1) [8,9,30]. The working fluid fill charge volume was 36 5 ml, corresponding to 61 % of the entire volume of the LHP, including the volumes of each component of the LHP presented in Table 1.

$$\alpha = \frac{\left(\frac{M_{charge}}{\rho_{l,start}}\right) - V_{ll} - V_{vl} - V_{c} - V_{e} - V_{w} - V_{D}}{V_{r}} \times 100 \quad (1)$$

The volume of each element constituting the LHP is determined during the design process, but the volume change due to the attachment of valves, various sensors, and fittings should be included in the total volume of the LHP. For this reason, the assembled LHP was weighed before and after it was filled with the working fluid. The total internal volume of the LHP was determined by comparing the two weights.

The thermocouples installed in the experimental device were *T*-type thermocouples of diameter 0.254 mm (AWG 30 gauge). As shown in Fig. 2, eight thermocouples (Nos. 1–8 in Fig. 2) and three thermocouples (Nos. 19–21 in Fig. 2) were welded to the outer wall surface of the evaporator and condenser, respectively. Two thermocouples were welded to measure the wall surface temperatures (Nos. 12 and 15 in Fig. 2) of the vapor and liquid transport tubes, respectively. The remaining thermocouples for measuring the temperature of the working fluid were probe-type thermocouples, inserted at the locations shown in Fig. 2. Before measurements were obtained, all thermocouples were calibrated between 0 and 300 °C, the measurement error being 0.5 °C. The entire LHP system was insulated with ceramic wool to minimize contact with the external environment. The thermal energy loss based on the energy balance between the thermal load and the amount of heat recovered by the condensing cooling source was estimated to be less than 10 % of the

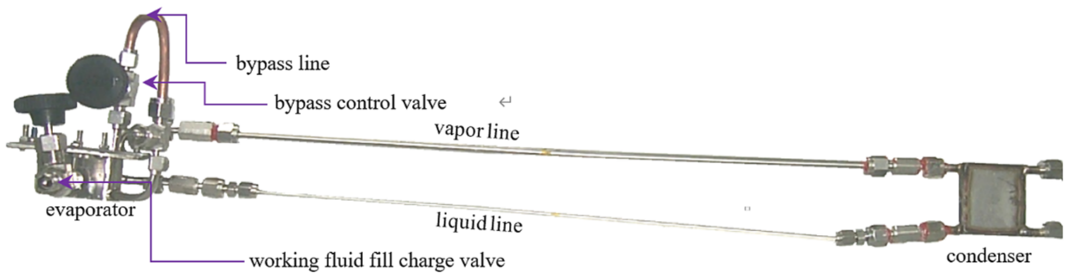

Fig. 5. Photo of the loop heat pipe with a bypass line that was used in this study.

Table 1
Internal volumes of LHP element [8,9].

LHP element	Volume (ml)	Phase
Condenser, V_c	5 7	Vapor/liquid
Vapor removal groove, V_g	4 1	Vapor
Wick, V_w	4 5	Vapor/liquid
Reservoir, V	35 5	Vapor/liquid
Liquid transport line, V_{ll}	1 57	Liquid
Vapor transport line, V_{vl}	6 8	Vapor
Bypass line, V_{bl}	1 8	Vapor

input thermal load [8].

The thermal load was controlled by a voltage controller and measured using a wattmeter with a maximum error of 0.5 %. The temperature and volume flow rate of the coolant were controlled using a thermal bath. During the experiment, the volume flow rate of the coolant was kept constant at 0.023 m^3/s (5 GPH) and was monitored using a rotameter with an error of up to 4 % for the full scale (10 GPH). Throughout the experiment, the coolant temperature was maintained at 10 °C. Table 2 lists the uncertainties and errors of the measuring instruments used in this study. The uncertainties were calculated using the measurement error indicated in the product catalog with reference to the literature [31]. The entire set of temperature data was read and stored every 2 s using a data acquisition device. Because all the experiments in this study focused on measuring whether the temperature overshoot for the evaporator could be controlled by the bypass line, the tilt angle of the LHP was the favorite angle (the condenser is located above the evaporator in the gravitational field; the arrow indicates the x–y coordinates in Fig. 2) of 15°, where the evaporator wall temperature overshoot was observed to be. In addition, as shown in Figs. 2 and 4, the liquid reservoir was always arranged to be located below the wick structure of the evaporator. The elements constituting the LHPs were washed with acetone to avoid contamination. The experiment was conducted in a well-equipped environment with heating and cooling facilities to maintain a constant internal temperature.

The heat recovered by the coolant was estimated by Eq. (2).

Table 2
Uncertainties of the instruments used in the experiment [8,9].

Independent variable	Error (gauge)	Uncertainty
Thermocouple (OMEGA, T-type, 30 AWG)	0.5 °C	0.00175
Thermal load (ISM, HD-301 M)	0.5 %	0.005
Isothermal bath (Teslab, RTE-111)	0.1 °C	0.000
Data acquisition system (Fluke, NetDAQ2640A)	0.01 %	0.0001
Flow meter (Dwyer, RMA-2)	0.5 cc	0.0

Thermocouple locations: 1–8: evaporator wall (T_w), 9: wick inlet ($T_{w,c..}$), 10: liquid reservoir (T_R), 11: evaporator outlet ($T_{\,o}$), 12: vapor line (T_{vl}), 13: condenser inlet (T_{ci}), 14: condenser outlet (T_{co}), 15: liquid line (T_{li}), 16: evaporator inlet (T_{ei}), 17: coolant inlet ($T_{cool.i}$), 18: coolant outlet ($T_{cool.o}$), 19–21: condenser wall (T_{cw}), 22: bypass line tube (T_{bl}).

$$Q_{out} = \left(\rho \dot{V} c\right)_{cool} (T_{cool.o} - T_{cool.i}) \quad (2)$$

where $T_{cool,i}$ and $T_{cool,o}$ are the inlet and outlet temperatures of the coolant, and $\dot{V}$ is the volumetric flow rate. The entire LHP device was properly insulated with ceramic wool to prevent thermal interaction with the surroundings. However, the thermal loss was less than 10 % based on the energy balance between the input thermal load in the evaporator and the thermal energy recovered through by the coolant from the condenser section. As shown in Fig. 6, the thermal loss increased with input thermal load (Q_{in}), and measured the minimum and maximum values of 1.1 % (at Q_{in} = 100 W) and 9.6 % (at Q_{in} = 260 W), respectively [8].

The purpose of this experiment was to investigate the possibility of temperature overshoot control by activating the bypass line in a situation where there was concern about damage to the temperature control object due to overheating when the temperature overshoot rose above 200 °C. Consequently, after applying the LHP to the input thermal load exceeding 160 W, the bypass valve was opened when the temperature overshoot increased by more than 200 °C. Three experiments were performed for each thermal load by specifying different bypass valve opening times. To prevent performance degradation of the working fluid, the operating temperature (thermocouple No. 11 in Fig. 2) was limited to 100 °C. In this experiment, an input thermal load of up to 270 W was applied, and the bypass valve was opened when the temperature overshoot rose above 200 °C after start-up under the NOM.

3. Results and discussion

The overshoot problems of LHPs can be found in previous studies [19–24] dealing with start-up characteristics. In these studies, the temperature overshoot was measured mainly in the horizontal arrangement of the LHP or in the favorite orientation assisted by gravity.

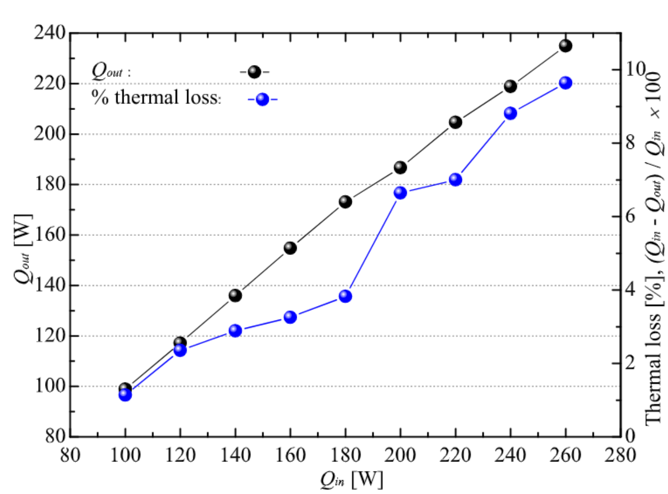

Fig. 6. Energy balance between the input thermal load and recovery heat [8].

Furthermore, the temperature overshoot may become larger [23] or smaller [19] with increasing input thermal load.

Fig. 7 shows the transient temperature history at the main points of the LHP measured under an input thermal load of 130 W at the horizontal orientation of the NOM. As shown in Fig. 7, the working of the LHP reached a steady state without any temperature overshoot within the entire input thermal load range. No temperature overshoot was observed in the horizontal slope.

In Figs. 8–13, figure number (a) shows the results of switching to the BOM by completely opening the bypass valve when the temperature overshoot on the evaporator wall rose above 200 °C after start-up in the NOM, figure number (b) shows the results of converting to the BOM before the temperature overshoot reached 200 °C, and figure number (c) shows the test result that reached the steady state by start-up using the BOM. When the bypass valve was opened and the bypass line activated, the wall surface temperature of the bypass line (temperature measured by thermocouple No. 22 in Fig. 1), T_{bl}, increased as the vapor flowed through the bypass line, T_{bl} being indicated by the bold red line. As shown in Fig. 2, since the input thermal load is supplied by a heater block with cartridge heaters mounted on the heat transfer surface of the evaporator wall, the evaporator wall temperature was measured to be the highest in these figures. Next, the temperature of the vapor region including the bypass tube wall temperature was measured to be high.

As shown in Refs. [8,9], T_{w3} (wall temperature measured through No. 3 thermocouple in Fig. 2) was measured to be the highest among the eight wall temperatures. Therefore, in the experimental results, the wall temperature overshoot control was presented based on the T_{w3}. Fig. 8 shows the experimental results for controlling the wall surface temperature overshoot of the evaporator using the bypass line under an input thermal load of 180 W. As shown in Fig. 8(a), after the LHP was started in the NOM, when the experimental time (t_1) was 5.2 min, the maximum temperature overshoot for the evaporator increased to 205 °C. The operation of the LHP was then switched to the BOM by opening the bypass valve. The overshoot of the evaporator wall temperatures decreased at the same time as T_{bl} increased under the BOM. When the experimental time (t_{s1}) passed 8.9 min, the temperatures of all locations of the LHP reached a steady state.

In the steady-state condition, the maximum temperature for the evaporator wall was measured to be 105.4 °C at T_{w3} (thermocouple No. 3 in Fig. 2). As shown in Fig. 8(b), when the conversion time (t_2) to the BOM was reduced to 1.5 min, the maximum temperature overshoot decreased to 153.6 °C. At this stage, the time to reach the steady-state condition (t_{s2}) was reduced to five min. The maximum temperature in the steady-state condition was measured to be approximately 101.4 °C,

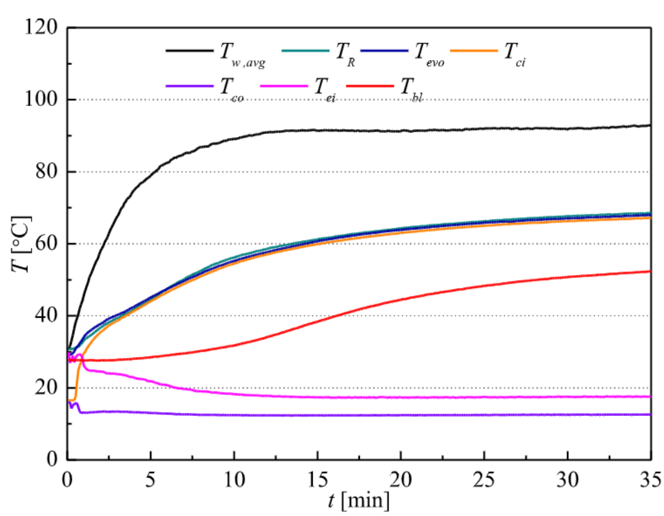

Fig. 7. Temperature history of the LHP with a thermal load of 130 W in horizontal orientation of the NOM.

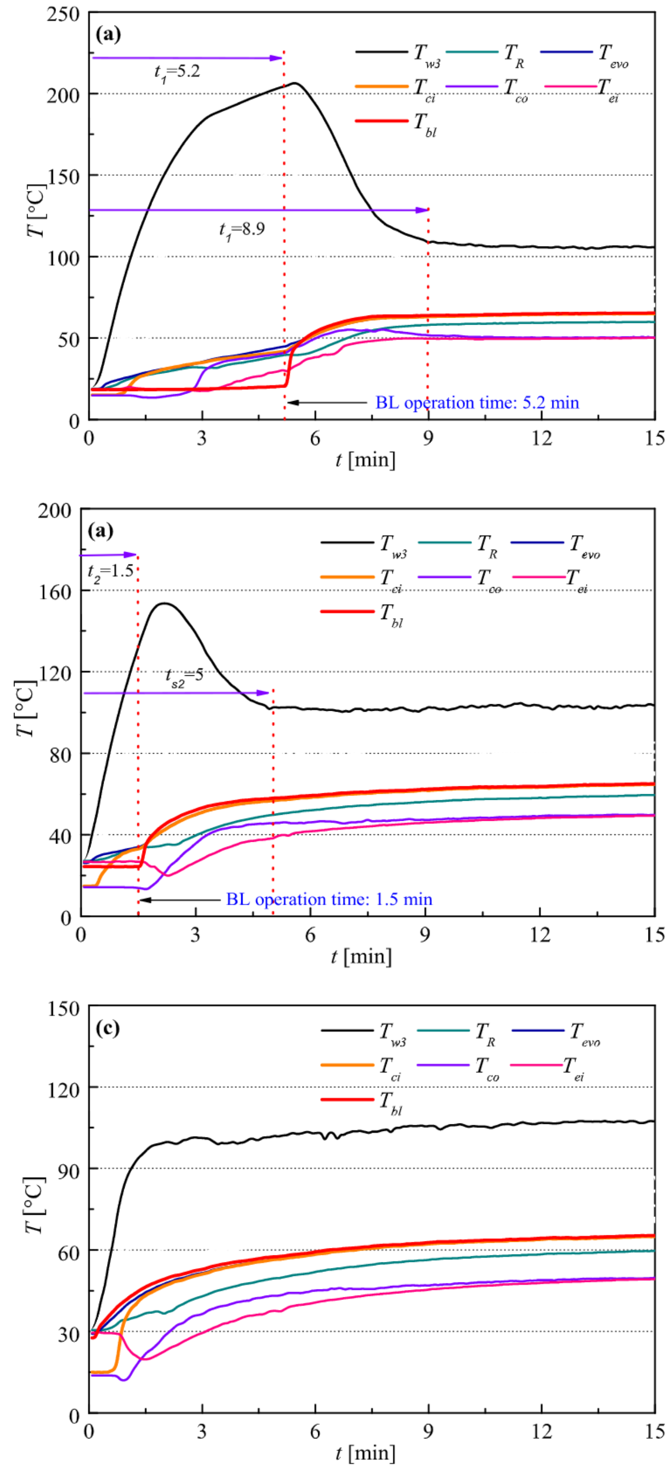

Fig. 8. Overshoot control of the LHP through the bypass line for (a) start-up time of 5.2 min, (b) start-up time of 1.5 min and (c) the BOM full start-up for a thermal load of 180 W.

and as the temperature overshoot decreased, the steady state wall temperature decreased by approximately 4 °C. As shown in Fig. 8(c), when the LHP was started using the BOM, the temperature overshoot of the evaporator wall was not measured.

Fig. 9 shows the results of controlling the temperature overshoot through the BOM while start-up in the NOM under 200 W of input thermal load, reaching the steady-state condition without a temperature overshoot after start-up in the BOM. When the experimental time (t_1)

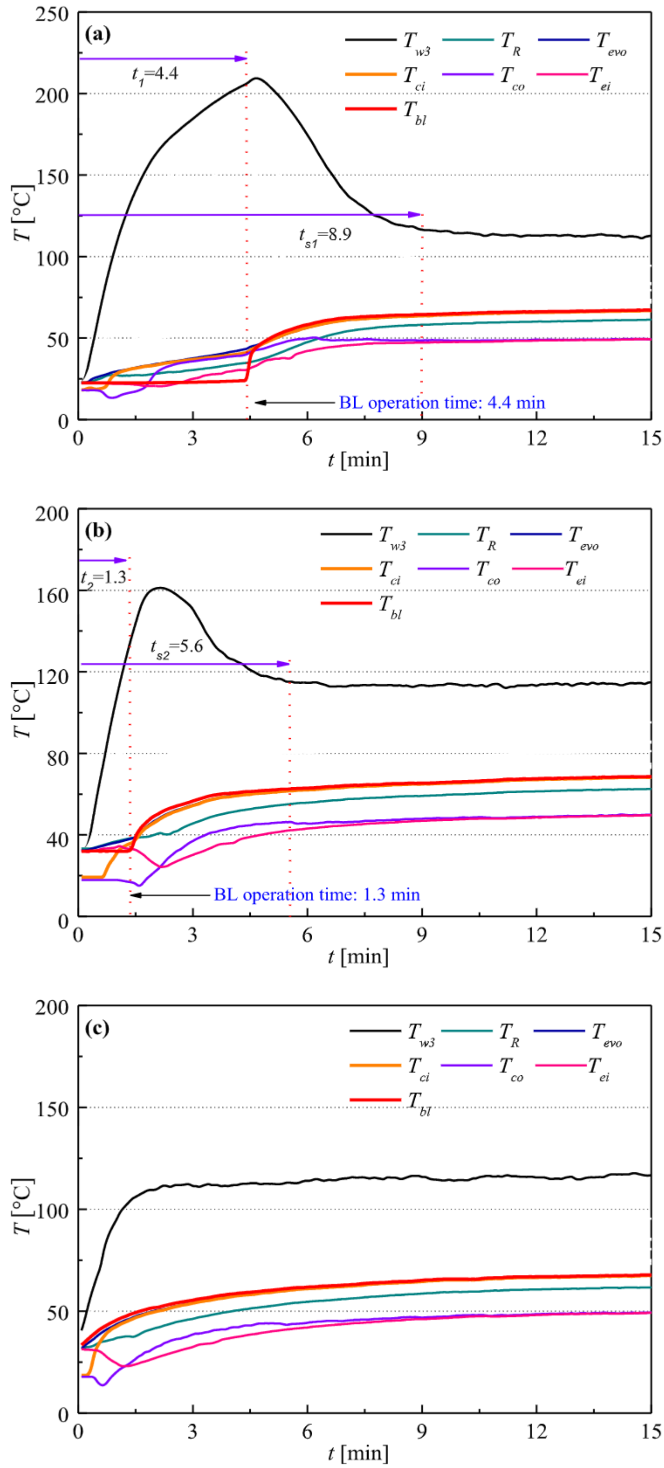

Fig. 9. Overshoot control of the LHP through the bypass line for (a) start-up time of 4.4 min, (b) start-up time of 1.3 min, and (c) the BOM full start-up for a thermal load of 200 W.

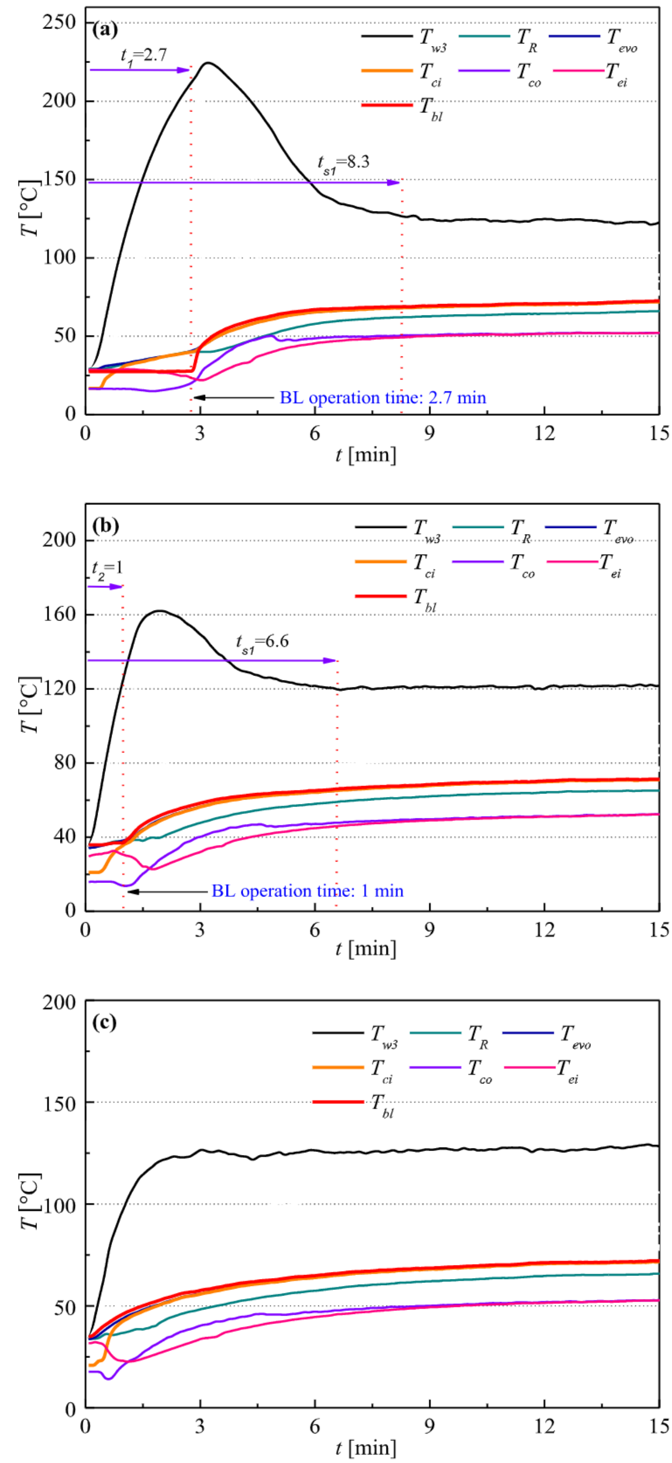

Fig. 10. Overshoot control of the LHP through the bypass line for (a) start-up time of 2.7 min, (b) start-up time of 1 min, and (c) the BOM full start-up for a thermal load of 220 W.

passed 4.4 min after starting in the NOM, the maximum temperature overshoot increased to 205 °C, the LHP operation being switched to the BOM. After the BOM conversion, a steady state was achieved after approximately 9 min (t_{s1}) as the temperature overshoot decreased. The maximum temperature of the evaporator wall was measured to be approximately 114 °C under steady-state conditions. As shown in Fig. 9(b), when the conversion time (t_2) to the BOM was reduced to 1.3 min, the maximum temperature overshoot decreased to 161 °C. When the steady-state condition was reached, the maximum temperature for the evaporator wall was measured to be 113.7 °C. As shown in Fig. 9(a), when the LHP was started in the BOM and reached a steady state, no temperature overshoot was observed.

Fig. 10 shows the results of the LHP, which was started in the NOM under an input thermal load of 220 W and converted to the BOM at times of 2.7 min (t_1 in Fig. 10(a)) and 1 min (t_2 in Fig. 10(b)), respectively. Fig. 10(c) shows the results after reaching the steady-state condition starting in the BOM. When time (t_1) elapsed, the bypass valve was

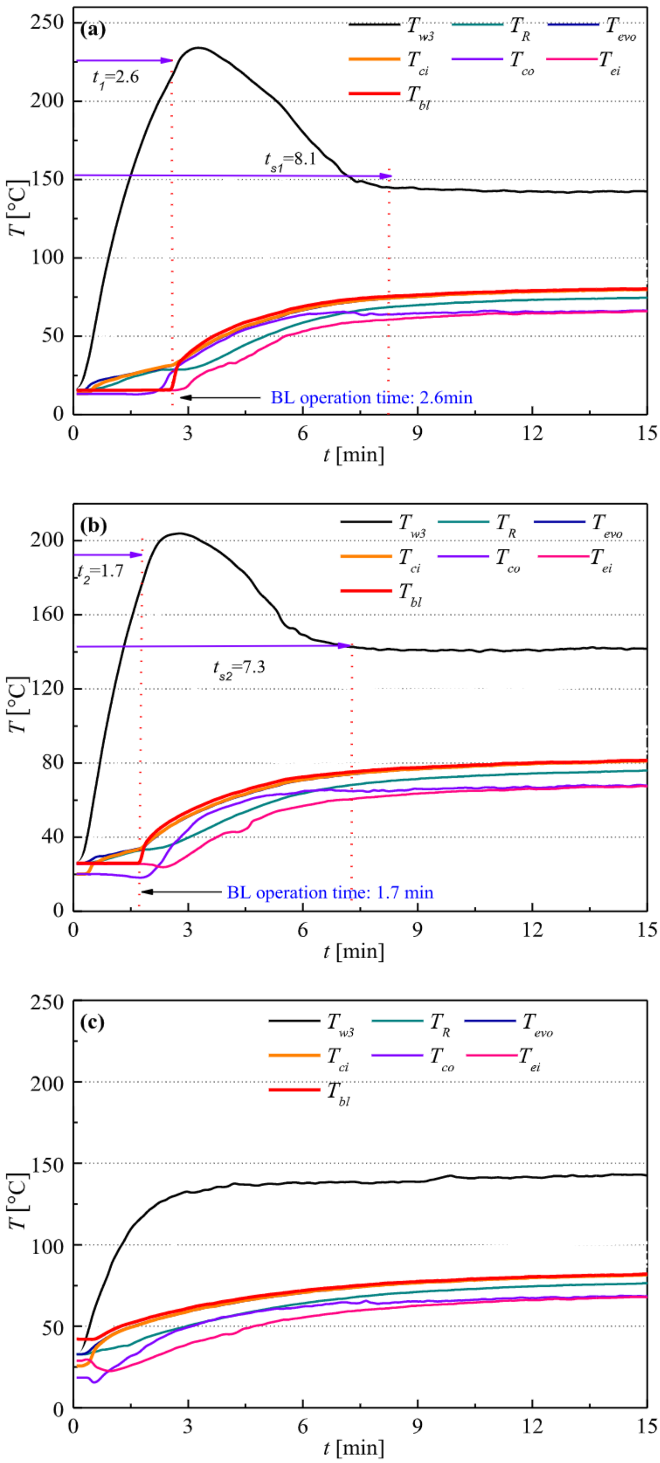

Fig. 11. Overshoot control of the LHP through the bypass line for (a) start-up time of 2.6 min, (b) start-up time of 1.7 min, and (c) the BOM full start-up for a thermal load of 240 W.

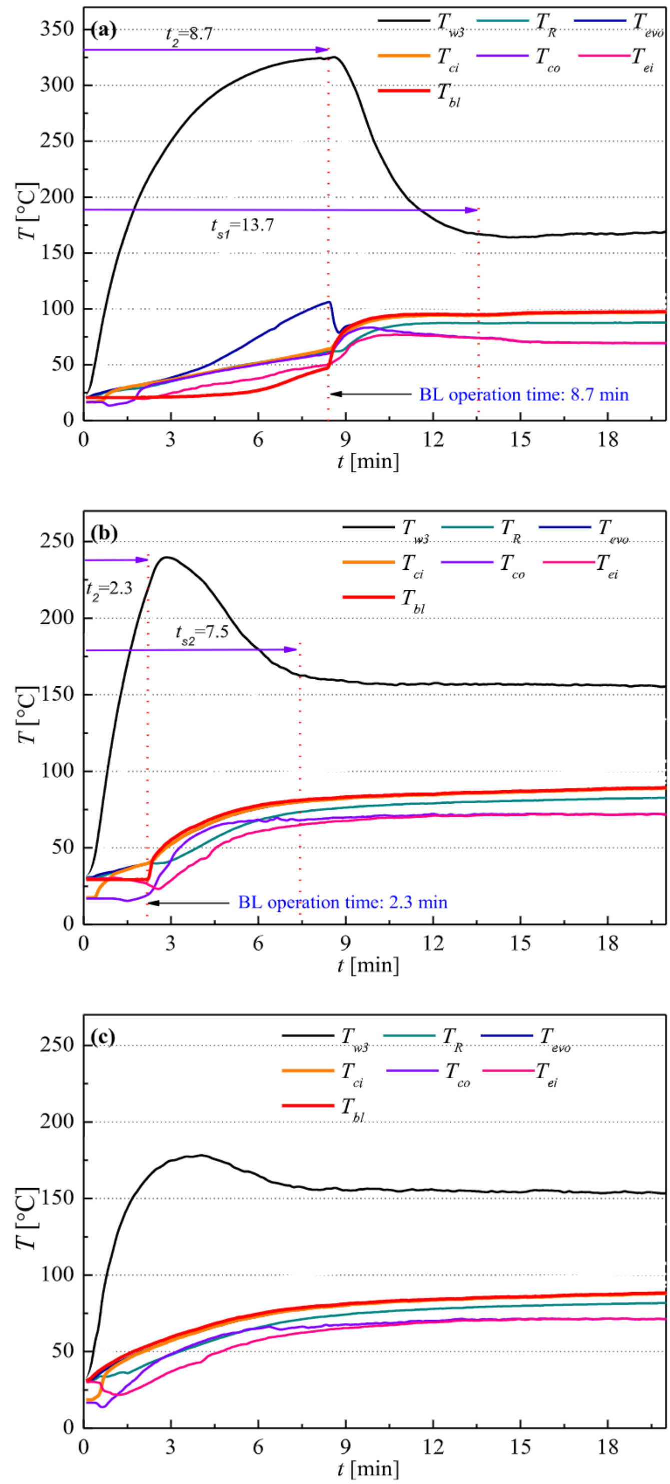

Fig. 12. Overshoot control of the LHP through the bypass line for (a) start-up time of 8.7 min, (b) start-up time of 2.3 min, and (c) the BOM full start-up for a thermal load of 260 W.

opened, T_{bl} increasing and the evaporator wall temperatures decreasing simultaneously. All temperatures reached a steady state after 8.3 min (t_{s1}). When the steady-state condition was achieved, the maximum temperature of the LHP was measured to be 124.5 °C. In the steady-state condition, T_{bl} and the vapor temperature were 70.4 and 74.3 °C, respectively, a difference of about 3.1 °C being measured. To measure the control performance for temperature overshoot in the BOM, the LHP operation was converted to the BOM 1 min after starting in the NOM. The maximum temperature overshoot was observed at 162 °C, the time (t_{s2}) to reach the steady state being reduced to 6.6 min. In the steady state condition, the maximum wall temperature of the evaporator was 122 °C. As shown in Fig. 10(c), when the LHP started in the BOM at an input thermal load of 220 W, the temperature overshoot problem could be avoided.

Fig. 11 shows the experimental results of controlling the temperature overshoot by increasing the input thermal load to 240 W. When converting to the BOM at 2.6 min (t_1) after starting in the NOM, the

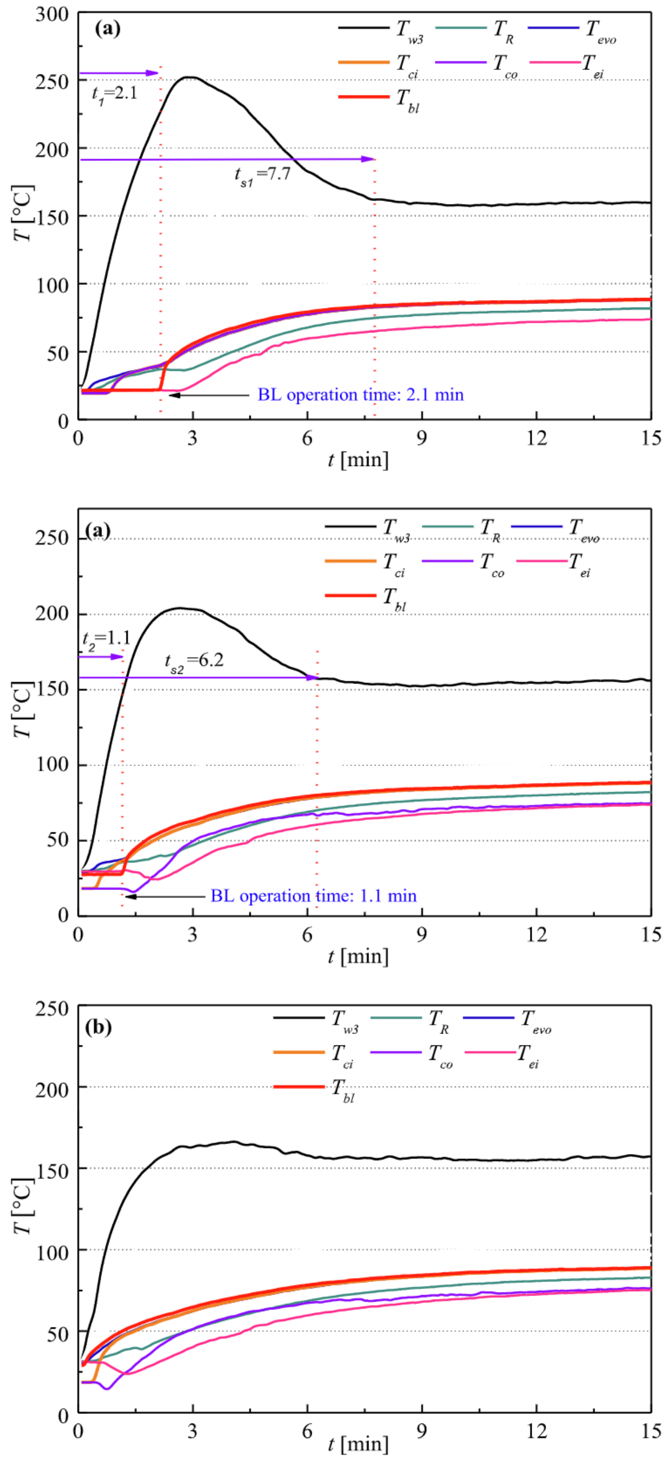

Fig. 13. Overshoot control of the LHP through the bypass line for (a) start-up time of 2.1 min, (b) start-up time of 1.1 min, and (c) the BOM full start-up for a thermal load of 270 W.

maximum overshoot temperature increased to 234.2 °C, and the steady-state condition was reached after an elapsed time of 8.1 min (t_{s1}). Under steady-state conditions, the maximum wall temperature of the evaporator was measured to be 141 °C. As shown in Fig. 11(b), when t_2 decreased by 0.9 min compared to t_1, the maximum temperature overshoot for the evaporator wall was lowered to 204 °C, and the time taken to reach the steady state (t_{s2}) was reduced by 0.8 min compared to t_{s1}. Under steady-state conditions, the maximum temperature for the evaporator wall was measured to be 141.5 °C. As shown in Fig. 11(c), even though the input thermal load was increased to 240 W, the BOM-based start-up could avoid the temperature overshoot phenomenon.

Fig. 12 shows the results of controlling the overshoot for the LHP evaporator wall temperature using the bypass line under an input thermal load of 260 W. As shown in Fig. 12(a), because the LHP operation was converted to the BOM only after 8.7 min (t_1), which was longer than in the other experiments, the temperature overshoot problem becomes serious. The maximum temperature overshoot for the evaporator wall increased to 325 °C, and the time (t_{s1}) taken to reach the steady state was delayed by 13.7 min. At this stage, the steady-state temperature was measured to be a maximum of 167.2 °C. However, when converting to the BOM after 2.3 min (t_2), the maximum temperature overshoot was 239.7 °C. The highest evaporator wall temperature was 156 °C under steady-state conditions, and the higher the wall temperature overshoot, the higher the steady-state temperature. When the LHP was started in the BOM under an input thermal load of 260 W, the temperature overshoot for the evaporator wall was measured, the maximum wall temperature during the start-up process being 176.7 °C.

Finally, Fig. 13 shows the results of controlling the temperature overshoot of the LHP using the BOM after applying an input thermal load of 270 W. As shown in Fig. 13(a), the BOM was applied to the LHP at $t_1 = 2.1$ min after starting in the NOM. The maximum temperature overshoot was measured to be 252.7 °C, and the time(t_{s1}) taken to reach the steady-state condition was estimated to be approximately 7.7 min. However, as shown in Fig. 13(b), when t_2 decreased by 1 min compared to t_1, the maximum temperature overshoot decreased by 48.3 °C compared to Fig. 13(a), t_{s2} being reduced by approximately 1.5 min compared to t_{s1}. As shown in Fig. 8(c), when the BOM was started under an input thermal load of 270 W, the evaporator wall temperature overshoot measured, the difference in the maximum wall temperature between the start-up and the steady state being less than 10.1 °C.

As shown in Figs. 8–13, the faster the BOM is applied, the lower the maximum temperature overshoot for the evaporator wall temperature, and accordingly, the shorter the time (t_s) to reach the steady-state condition. As mentioned in Ref. [9], the vapor produced during LHP start-up in the BOM cannot escape the vapor channel because of insufficient capillary force; therefore, the stagnant vapor inside the evaporator is quickly discharged through a short bypass line. In other words, while the LHP is starting, the circulation of the working fluid inside the evaporator can be accelerated by the BOM. Therefore, the possibility for passive control of the temperature overshoot of the LHP was obtained. Furthermore, if an active control method for the bypass control valve is provided, it can be evaluated that the bypass line can function as a safety device of the LHP. From these results, the bypass line can be a useful control device such that the maximum temperature of the LHP does not exceed a specific temperature during the LHP start-up and under steady-state conditions. As mentioned in Ref. [8], the bypass line had a negative effect on the heat transfer performance of LHP under certain conditions, low thermal load. From the result of Figs. 8–13, if the bypass line is designed to be activated only when the evaporator wall temperature exceeds a certain temperature level, the bypass line can be a useful way to function as an emergency safety device of the LHP.

Fig. 14 shows the results of converting to the BOM 2.42 min after starting by applying the NOM under an input thermal load of 270 W and changing back to the NOM after 49.3 min. When the NOM was started, the evaporator wall temperature overshoot increased to 253.3 °C. When the bypass valve was opened during start-up, the LHP operation achieved a steady state with an increase in the wall temperature ($T_{b\,l}$) of the bypass tube and a simultaneous decrease in the evaporator wall temperatures. Under steady-state operation in the BOM, the maximum evaporator wall temperature was 168.3 °C. After 49.3 min, the LHP operation was converted to the NOM once again, and the maximum evaporator wall temperature rose to approximately 201 °C. A physical description of the steady-state heat transfer performance of LHPs under high thermal load and BOM operation is provided in Ref. [8].

Fig. 15 shows the control performance index on the temperature

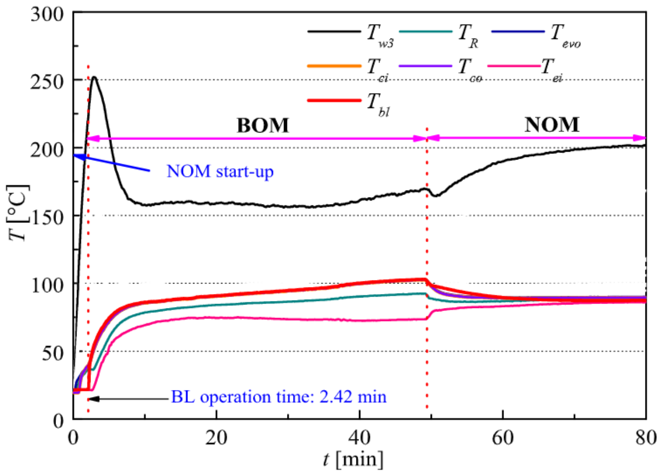

Fig. 14. Start-up and steady-state characteristics of the LHP in the BOM and NOM for a thermal load of 270 W.

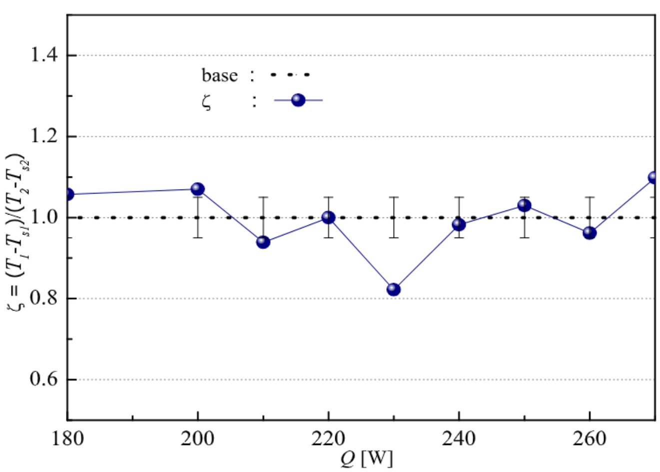

Fig. 15. Investigation of overshoot control performance index based on the input thermal load.

overshoot of the bypass line based on the input thermal load. The temperature overshoot control performance index can be expressed as Eq. (3).

$$\zeta = \frac{t_1 - t_{s1}}{t_2 - t_{s2}} \tag{3}$$

As the physical meaning of Eq. (3), this indicator includes the dependence on the time at which the LHP reaches a steady state and the time at which the BOM is applied. As shown in Figs. 8–13, the faster the BOM is applied during the start-up of the LHP with temperature overshoot, the shorter the time it takes for the temperature to reach the steady-state condition. When ζ is close to 1, the time difference between reaching the steady-state condition and applying the BOM may be constant regardless of the time taken to apply the BOM. In other words, as ζ approaches 1, it can be guaranteed that the reliability increases when the bypass line is applied as an emergency safety device to the LHP system. As shown in Fig. 15, for most input thermal loads, ζ approaches 1 within a 5 % margin, but in the case of a 230 W input thermal load, the marginal difference was approximately 8 %.

4. Conculsions

Normal start-up of the LHP can be difficult or even impossible because overshoot problems for the evaporator temperature of the LHP at high thermal loads can be serious. In this study, we examined temperature overshoot control by applying a bypass line under high input thermal loads, ranging from 180 to 270 W. Three experiments were conducted under these thermal loads.

(1) When the temperature overshoot rose above 200 °C after starting in the NOM, the temperature overshoot was controlled by applying the BOM.
(2) By shortening the BOM application time, the bypass valve was opened at any stage before the temperature overshoot reached 200 °C.
(3) Test results in which the LHP was started in the BOM and reached a steady-state condition were presented.

The temperature overshoot problem occurring in the LHP starting in the NOM could be effectively controlled using the BOM. Moreover, the time difference between the application of the BOM and the arrival of the steady-state condition was maintained under all input thermal loads, confirming the reliability of temperature overshoot control using the bypass line. When the LHP was started in the BOM under an input thermal load of 240 W or less, the temperature overshoot was not measured, but when the input thermal load increased to 250 W or more, a weak temperature overshoot was measured. When the bypass line was applied to the LHP, control of the temperature overshoot was possible during start-up. A strong reliability was obtained for passive control of the temperature overshoot of the LHP. Furthermore, if an active control method for the bypass control valve is provided, the bypass line can function as a safety device of the LHP. Consequently, if the bypass line is applied only to prevent overheating during start-up in the LHP system, it can function as an LHP safety device.

Declaration of Competing Interest

The authors declare that they have no known competing financial interests or personal relationships that could have appeared to influence the work reported in this paper.

Data availability

No data was used for the research described in the article.

Acknowledgment

This research was supported by a National Research Foundation of Korea (NRF) grant (No. NRF-2018R1D1A1B07040929, No. NRF-2022R1F1A1066459 and No. NRF-2022R1A2C1009690) funded by the Korean government (MSIT).

References

[1] M.C. Page, Modeling and experimental validation of a loop heat pipe for terrestrial thermal management applications, University of KwaZulu-Natal MS dissertation, 2013.
[2] S. Lei, Y. Shi, G. Chen, Heat pipe based spray-cooling thermal management system for lithium-ion battery: Experimental study and optimization, Int. J. Heat Mass Transf. 163 (2020), 120494.
[3] H. Behi, D. Karimi, M. Behi, M. Ghanbarpour, J. Jaguem, M.A. Sokkeh, F. H. Gandoman, M. Berecibar, J. Mierlo, A new concept of thermal management system in Li-ion battery using air cooling and heat pipe for electric vehicles, Int. J. Heat Mass Transf. 174 (2020), 115280.
[4] B. Ariantara, N. Putra, S. Supriadi, Battery thermal management system using loop heat pipe with LTP copper capillary wick, IOP Conference Series: Earth and Environmental Science 105 (2018), 012045.
[5] J.H. Boo, E.G. Jung, Bypass line assisted start-up of a loop heat pipe with a flat evaporator, J. Mech. Sci. Technol. 23 (2009) 1613–1619.
[6] Z. Hongxing, L. Guiping, D. Ting, Y. Wei, S. Xingguo, R.G. Sudakov, Y.F. Maidanik, Investigation on Startup Behaviors of a Loop Heat Pipe, J. Thermophys Heat Transfer 19 (2005) 509–518.
[7] Y.F. Maydanik, Loop heat pipes, Appl. Therm. Eng. 25 (5-6) (2005) 635–657.
[8] E.G. Jung, J.H. Boo, Experimental observation of thermal behavior of a loop heat pipe with a bypass line under high heat flux, Energy 197 (2020), 117242.

[9] E.G. Jung, J.H. Boo, Overshoot elimination of the evaporator wall temperature of a loop heat pipe through a bypass line, Appl. Therm. Eng. 165 (2020), 114594.
[10] B. Mo, M.M. Ohadi, S.V. Dessiatoun, K.R. Wrenn, Capillary Pumped-Loop Thermal Performance Improvement with Electrohydrodynamic Technique, J. Thermophys Heat Transfer 14 (2000) 103–108.
[11] B. Mo, M.M. Ohadi, S.V. Dessiatoun, K.H. Cheung, Startup Time Reduction in an Electrohydrodynamically Enhanced Capillary Pumped Loop, J. Thermophys Heat Transfer 13 (1999) 134–139.
[12] L. Liu, X. Yang, B. Yuan, Y. Zhang, J. Wei, Experimental study of a novel loop heat pipe with a vapor-driven jet injector, Int. J. Heat Mass Transf. 164 (2021), 120518.
[13] L. Liu, X. Yang, B. Yuan, X. Ji, J. Wei, Experimental study on thermal performance of a loop heat pipe with a bypass line, Int. J. Heat Mass Transf. 147 (2020), 118996.
[14] I. Muraoka, F.M. Ramos, V.V. Vlassov, Analysis of the operational characteristics and limits of a loop heat pipe with porous element in the condenser, Int. J. Heat Mass Transf. 44 (12) (2001) 2287–2297.
[15] T.S. Zhao, Q. Liao, On capillary-driven flow and phase-change heat transfer in a porous structure heated by a finned surface: Measurements and modeling, Int. J. Heat Mass Transf. 43 (2000) 1141–1155.
[16] Y.M. Baek, E.G. Jung, Heat transfer performance of loop heat pipe for space vehicle thermal control under bypass line operation, Int. J. Heat Mass Transf. 194 (2022), 123064.
[17] D. Khrustalev, A. Faghri, Heat transfer in the inverted meniscus type evaporator at high heat fluxes, Int. J. Heat Mass Transf. 38 (16) (1995) 3091–3101.
[18] D. Khrustalev, A. Faghri, Estimation of the maximum heat flux in the inverted meniscus type evaporator of a flat miniature heat pipe, Int. J. Heat Mass Transf. 39 (9) (1996) 1899–1909.
[19] L. Bai, Y. Tao, Y. Guo, G. Lin, Startup characteristics of a dual compensation chamber loop heat pipe with an extended bayonet tube, Int. J. Heat Mass Transf. 148 (2020), 119060.
[20] J. He, J. Miao, L. Bai, G. Lin, H. Zhang, D. Wen, Effect of non-condensable gas on the startup of a loop heat pipe, Appl. Therm. Eng. 111 (2017) 1507–1516.
[21] L. Bai, G. Lin, D. Wen, J. Feng, Experimental investigation of startup behaviors of a dual compensation chamber loop heat pipe with insufficient fluid inventory, Appl. Therm. Eng. 29 (8-9) (2009) 1447–1456.
[22] Y. Qu, D. Zhou, S. Qiao, K. Zhou, Y. Tian, Experimental study on the startup performance of dual-evaporator loop heat pipes, Int. J. Therm. Sci. 170 (2021), 107168.
[23] Z. Yang, Y. Zhang, L. Bai, H. Zhang, G. Lin, Experimental study on the thermal performance of an ammonia loop heat pipe using a rectangular evaporator with longitudinal replenishment, Appl. Therm. Eng. 207 (2022), 118199.
[24] X. Wang, J. Wei, Visual investigation on startup characteristics of a novel loop heat pipe, Appl. Therm. Eng. 105 (2016) 198–208.
[25] Z.C. Liu, W. Liu, A. Nakayama, Flow and heat transfer analysis in porous wick of CPL evaporator based on field synergy principle, Heat Mass Transf. 43 (2007) 1273–1281.
[26] V.G. Pastukhov, Y.F. Maidanik, C.V. Vershinin, M.A. Korukov, Miniature loop heat pipes for electronics cooling, Appl. Therm. Eng. 23 (9) (2003) 1125–1135.
[27] G.P. Celata, M. Cumo, M. Furrer, Experimental tests of a stainless-steel loop heat pipe with flat evaporator, Exp. Therm Fluid Sci. 34 (7) (2010) 866–878.
[28] Y.F. Maydanik, M.A. Chernysheva, V.G. Pastukhov, Review: Loop heat pipes with flat evaporators, Appl. Therm. Eng. 67 (2014) 294–307.
[29] N. Atabaki B.R. Baliga Experimental investigation of a loop heat pipe with a flat evaporator, in 2006 Sidney. Australia.
[30] H. Mohammed, C. Debra, M. Praveen, S. Ahmed, M.G. Frank, H.T. Henderson, E. Golliher, K. Mellott, C. Moore, Loop heat pipe (LHP) development by utilizing coherent porous silicon (CPS) wicks, Inter Society Conference on Thermal Phenomena (2002) 457–463.
[31] J.P. Holman, Experimental methods for engineers, McGraw-Hill, 1996.